

# The Fold-In Approach to Bowl-Shaped Aromatic Compounds: Synthesis of Chrysaoroles\*\*

Damian Myśliwiec and Marcin Stępień\*

The chemistry of bowl-shaped aromatic compounds, known as buckybowl and geodesic polyarenes, is an area of significant theoretical and practical interest.<sup>[1]</sup> The current extensive research on these systems has been largely motivated by their structural relationship to fullerenes and carbon nanotubes. Indeed, all-carbon buckybowl, such as corannulene<sup>[1b,c,e,2]</sup> and sumanene,<sup>[1d,3]</sup> can be viewed as nanotube end caps or fullerene sections, and have been explored as templates for controlled syntheses of well-defined molecular forms of elemental carbon.<sup>[4]</sup> However, the interest in bowl-shaped aromatic compounds extends beyond the quest for new carbon-rich materials and encompasses aspects of their internal strain,<sup>[5]</sup> aromaticity,<sup>[6]</sup> metal coordination,<sup>[1d,7]</sup> and supramolecular chemistry.<sup>[1e]</sup> All these facets of research create the need for new structural motifs and synthetic methodologies.<sup>[1f,8]</sup>

The crucial points in every synthesis targeting a bowl-shaped aromatic structure are the choice of chemical reactivity capable of incorporating strain into the  $\pi$ -electron system being constructed, and the placement of the strain-inducing step in the overall synthetic plan. In the synthesis of corannulene by Lawton and Barth,<sup>[2]</sup> the bowl was constructed by multiple annulations around the central five-membered ring. In the final step, responsible for the introduction of strain, a partly saturated corannulene precursor was subjected to catalytic dehydrogenation to yield the target molecule. Strain buildup was similarly postponed until the final synthetic step in the first successful preparation of sumanene.<sup>[3]</sup> However, in many contemporary syntheses of corannulene and higher geodesic hydrocarbons,<sup>[1,4,8]</sup> unsaturated rings have been closed efficiently with the concomitant introduction of strain. This approach has been successful with a number of specialized reaction types, most notably high-temperature pyrolysis and metal-mediated coupling.<sup>[1b,c,e]</sup> Interestingly, all of the above approaches rely on a common “stitching”<sup>[1f]</sup> tactic: the bowl is elaborated from the center

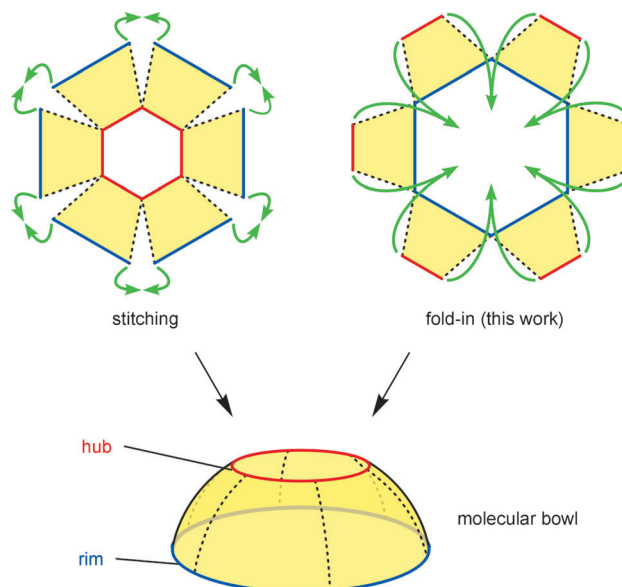


Figure 1. Synthetic approaches to bowl-shaped aromatic compounds.

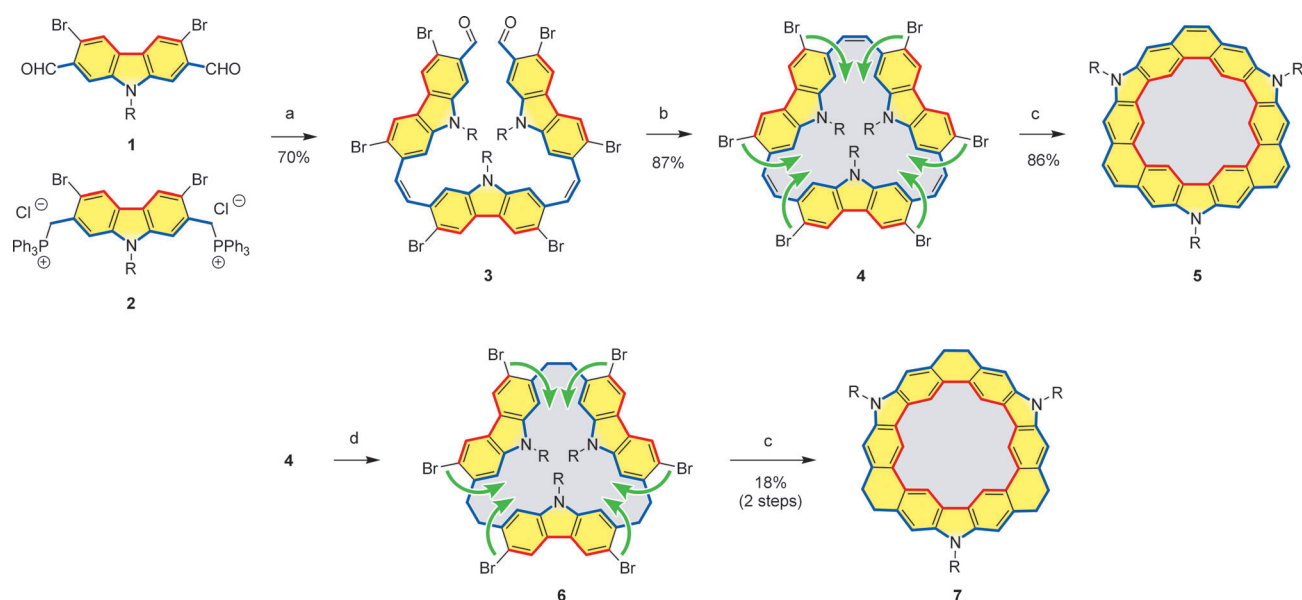
(“hub”) towards the rim (Figure 1). One can envisage a complementary strategy, which begins with a macrocyclic precursor containing the complete rim of the bowl. The precursor will consist of a number of aromatic subunits (shown as yellow trapezoids in Figure 1), which can be “folded in” and coupled so as to complete the central part of the bowl. A fold-in synthesis is potentially difficult to design, because its outcome will depend not only on the geometrical matching of subunits but also on the extent of conformational flexibility of the macrocycle, and this conformational flexibility may change in the course of the folding process. However, by reversing the sequence of bond formation in the fold-in synthesis, different reactivity patterns that could lead to otherwise inaccessible systems may be explored. To test the viability of the fold-in approach, we selected carbazole-based bowls as initial targets. Our choice was motivated by geometrical and reactivity considerations and, in part, by the scarcity of bowl-shaped heteroaromatic compounds.<sup>[9]</sup>

Our reaction sequence starts with two carbazole derivatives (Scheme 1): the dialdehyde **1** and bis(phosphonium) salt **2**, which were prepared from 2,7-dibromocarbazole as described in the Supporting Information. The treatment of **2** with dialdehyde **1** (4 equiv) under Wittig conditions yielded tricarbazole **3** in 70% yield. This reaction proceeded with good *Z* selectivity owing to the beneficial effect of *ortho* halogen substituents.<sup>[10]</sup> However, the *Z,Z* isomer of **3** is highly photosensitive and undergoes rapid isomerization to the insoluble *E,E* form in ambient light. The use of excess

[\*] D. Myśliwiec, Dr. M. Stępień  
Wydział Chemii, Uniwersytet Wrocławski  
ul. F. Joliot-Curie 14, 50-383 Wrocław (Poland)  
E-mail: marcin.stepien@chem.uni.wroc.pl  
Homepage: <http://www.mstepien.edu.pl>

[\*\*] Financial support from the National Science Center (grant N N204 199340) is gratefully acknowledged. Quantum-chemical calculations were performed in the Wrocław Center for Networking and Supercomputing. We thank Prof. Tadeusz Lis for solving the X-ray crystal structure of **4** and for helpful discussions. We thank Dr. Piotr Stefanowicz and Dr. Piotr Jakimowicz for their assistance with mass spectrometry.

Supporting information for this article is available on the WWW under <http://dx.doi.org/10.1002/anie.201208547>.



**Scheme 1.** Synthesis of chrysaoroles **5** and **7** ( $R = n\text{Bu}$ ): a) aqueous NaOH,  $\text{CH}_2\text{Cl}_2$ , 1 h,  $Z,Z/Z,E \approx 4:1$ ; b)  $\text{TiCl}_4$ , Zn, CuI, THF, reflux, 12 h, slow addition; c)  $[\text{Ni}(\text{cod})_2]$ , 1,5-cyclooctadiene, 2,2'-bipyridyl, DMF/toluene,  $85^\circ\text{C}$ , 18 h; d)  $\text{H}_2$ ,  $\text{PtO}_2$ ,  $\text{CH}_2\text{Cl}_2$ ,  $20^\circ\text{C}$ . cod = 1,5-cyclooctadiene, DMF = *N,N*-dimethylformamide.

dialdehyde **1** in the synthesis of **3** is helpful in minimizing the extent of polymerization. The macrocyclization of **3** by McMurry coupling under pseudo-high-dilution conditions provided carbazolophane **4** in 87% yield. The direct cyclotrimerization of **1** under McMurry conditions was also explored as a potentially simpler route to **4**, but this alternative procedure suffered from lower yields (ca. 8%) and purification difficulties.

The structure of **4**, the first macrocycle en route to the bowl-shaped target, was of significant interest. The inspection of molecular models had shown that multiple substitution of the cyclophane (bromine atoms and butyl chains) might hinder the rotation of the carbazole rings in the macrocyclic frame and thus result in the formation of atropisomers. With three equivalent subunits in a cyclic arrangement, two atropisomers are possible:  $\alpha\alpha\alpha$ , with three *N*-butyl chains on one side of the macrocyclic plane, and  $\alpha\alpha\beta$ , with one of the chains on the opposite side. X-ray crystallographic analysis of **4**<sup>[11]</sup> revealed that  $\alpha\alpha\beta$  is the preferred arrangement in the solid state (Figure 2). In fact, the three carbazole units are quite sharply tilted relative to the mean plane of the vinylene

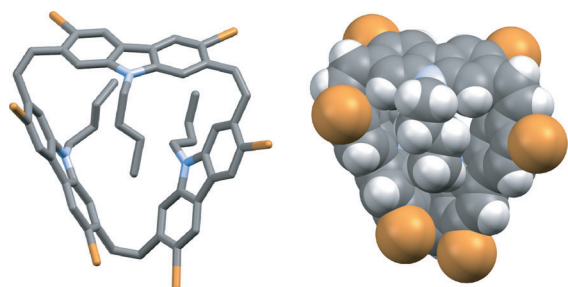


**Figure 2.** Observed molecular structure of **4** in the solid state. Solvent molecules, disordered butyl chains, and hydrogen atoms (in the stick model) are omitted for clarity.

bridges, with interplanar angles of  $49$ ,  $91$ , and  $-81^\circ$ . The carbazole moieties are themselves nearly planar, which indicates that in spite of the internal crowding, the structure is relatively unstrained. The  $^1\text{H}$  NMR spectrum of **4**, recorded in  $\text{CDCl}_3$  at  $298\text{ K}$ , reveals threefold effective molecular symmetry, which is consistent with either the prevalence of the  $\alpha\alpha\alpha$  structure in solution or rapid conformational exchange involving the  $\alpha\alpha\beta$  form. Preliminary DFT calculations on the two conformers indicated that the  $\alpha\alpha\beta$  form is more stable than  $\alpha\alpha\alpha$  by approximately  $11\text{ kcal mol}^{-1}$  and thus lend support to the latter hypothesis. Variable-temperature  $^1\text{H}$  NMR spectra of **4** ( $600\text{ MHz}$ ,  $\text{CD}_2\text{Cl}_2$ ) showed gradual line broadening below  $190\text{ K}$ ; however, the coalescence point could not be reached above  $160\text{ K}$ . Although inconclusive, this observation is also consistent with the presence of the  $\alpha\alpha\beta$  form in solution and its rapid conformational exchange involving the  $\alpha\alpha\alpha$  form.

In the final synthetic step, we subjected **4** to an Ullmann-type coupling in the presence of zerovalent nickel<sup>[12]</sup> with the intention of forming three new C–C bonds and completing the hub of the molecule. This fold-in transformation proved successful, and 9,18,45-tributylchrysaorole (**5**) was isolated in 86% yield after chromatographic workup. Chrysaorole<sup>[13,14]</sup> **5**, a yellow compound with yellow-green fluorescence, has limited stability in solution, but solid samples can be stored for weeks in the refrigerator. Compound **5** shows a characteristically simple  $^1\text{H}$  NMR spectrum (Figure 3), which reflects its high molecular symmetry ( $C_{3v}$ ). The spectrum contains a signal at  $\delta = 9.42\text{ ppm}$  assigned to the hub hydrogen atoms, two signals at  $\delta = 7.59$  and  $7.33\text{ ppm}$  due to the hydrogen atoms at the rim, and a set of resonances corresponding to the three equivalent butyl chains. Although the downfield signals appear as singlets, a weak remote coupling was identified in the COSY spectrum between the lines at  $\delta = 9.42$  and  $7.33\text{ ppm}$  ( $^5J < 1\text{ Hz}$ ). To complete the assignment, we noted

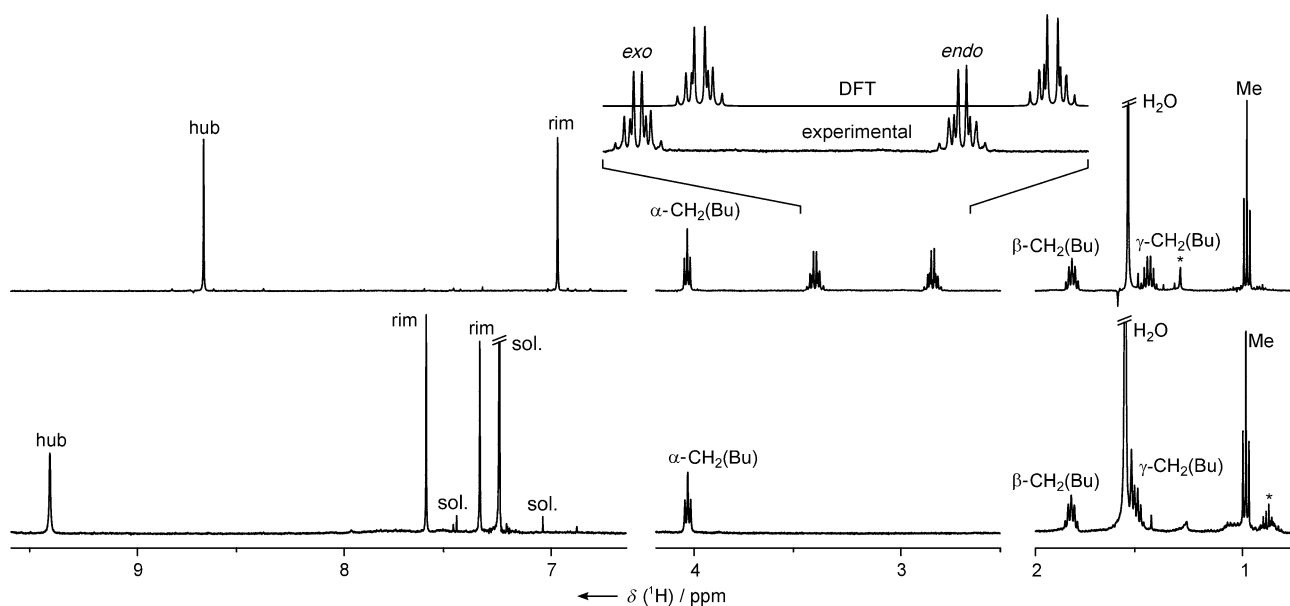


**Figure 3.**  $^1\text{H}$  NMR spectra of chrysaorole **5** (500 MHz,  $\text{CDCl}_3$ , 300 K, bottom) and hexahydrochrysaorole **7** (500 MHz,  $\text{CD}_2\text{Cl}_2$ , 300 K, top). The inset shows the simulated multiplet structure of *endo* and *exo* signals as derived from the DFT calculation of coupling constants. sol. = solvent.

in the ROESY map that the signal at  $\delta = 7.59$  ppm yields a dipolar coupling not only with the other rim signal but also with the  $\alpha\text{-CH}_2$  resonance. The  $^{13}\text{C}$  NMR spectrum of **5** contains seven signals in the region of  $\text{sp}^2$  carbon atoms, in agreement with the proposed structure. HSQC and HMBC spectra enabled the complete assignment of the  $^{13}\text{C}$  resonances of **5** (see the Supporting Information).

Further insight into the three-dimensional structure of **5** was obtained from DFT calculations performed at the B3LYP/6-31G\*\* level of theory.<sup>[15]</sup> In the optimized model, the fused chrysaorole skeleton shows the expected bowl-like curvature distributed quite evenly over the constituent rings (Figure 4). Because of the nonplanarity of the system, each of the butyl chains can adopt two nonequivalent orientations that differ by rotation by  $180^\circ$  about the N–C bond: “pendant” (shown in Figure 4) and “outstretched”. These two orientations are predicted to be effectively isoenergetic (see the Supporting Information). Rotamer-averaged  $^1\text{H}$  and  $^{13}\text{C}$  nuclear-shielding values calculated by the GIAO method are in excellent agreement with experimental data (Figure 5). This good correlation indicates that the optimized DFT structure is in quantitative agreement with the actual molecular geometry.<sup>[16]</sup>

Chrysaorole differs from typical buckybowls in that its hub consists of a uniquely large, 18-membered ring.<sup>[17]</sup> However, the presence of six hydrogen atoms in the hub makes the remaining opening quite small. The depth of the bowl, as measured from the level of hub carbon atoms to the rim, is 1.96 Å, and thus larger than the depth of corannulene (0.87 Å<sup>[18]</sup>). The pyramidalization of  $\text{sp}^2$  centers in chrysaorole, as measured on the basis of  $\pi$ -orbital-axis-vector (POAV) inclination angles ( $\theta$ ),<sup>[19]</sup> is smaller than that observed for most geodesic polyarenes, but the distribution of values over specific positions in the structure follows a similar trend. In particular, small  $\theta$  values ( $1\text{--}2^\circ$ ) are observed for tertiary

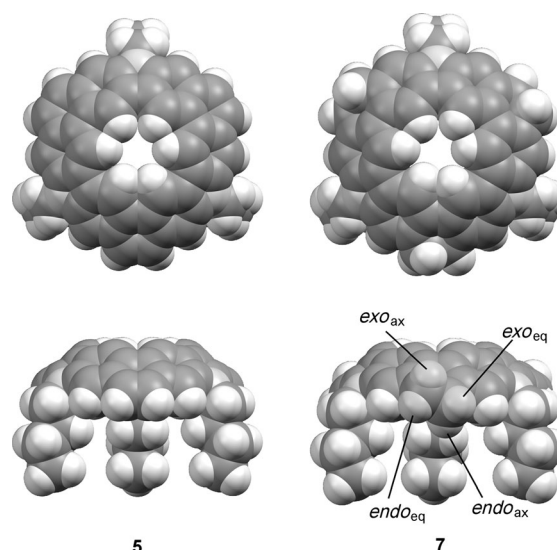


**Figure 4.** DFT-optimized structures of 9,18,45-tributylchrysaorole (**5**;  $\text{C}_{3v}$  conformer with pendant chains) and 9,18,45-tributyl hexahydrochrysaorole (**7**;  $\text{C}_3$  conformer with pendant chains). The labeling of ethylene hydrogen atoms is shown for **7**.

centers, whereas the largest inclinations ( $\theta = 4\text{--}5^\circ$ ) occur at the quaternary carbon atoms that form the hub. Interestingly, even though they are located on the rim, the nitrogen atoms show a fair degree of pyramidalization, which is dependent on the assumed orientation of the butyl chains ( $\theta = 3.7\text{--}5.8^\circ$ ). A strain energy of  $53.4 \text{ kcal mol}^{-1}$  was estimated for the unsubstituted chrysaorole (**5a**,  $\text{R} = \text{H}$ , B3LYP/6-31G\*\*) on the basis of the homodesmotic reaction shown in Scheme 2. This value is significantly higher than the estimate given for corannulene ( $24.2 \text{ kcal mol}^{-1}$ ), but the amount of strain per

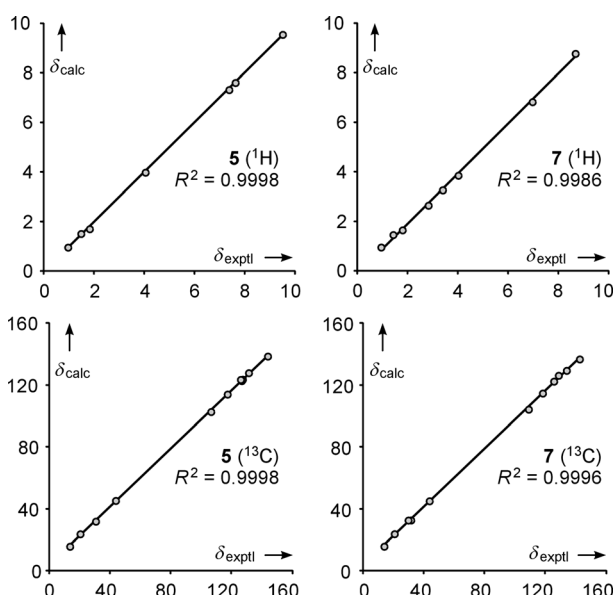
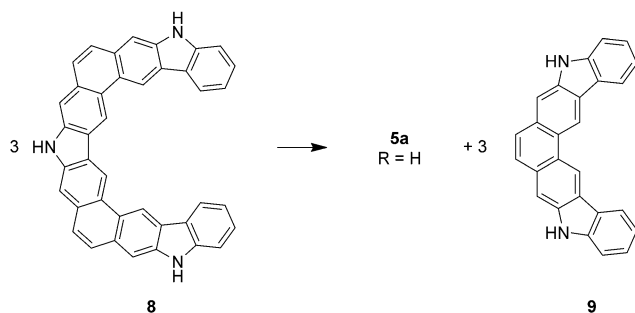


**Figure 5.** Correlation between the rotamer-averaged  $^1\text{H}$  and  $^{13}\text{C}$  chemical shifts calculated for **5** and **7** (GIAO/B3LYP/6-31G(d,p),  $\delta_{\text{calc}}$ ) and the corresponding experimental values ( $\delta_{\text{exptl}}$ ). See the Supporting Information for details.



**Scheme 2.** Homodesmotic reaction used to estimate the strain energy in chrysaorole.

$\text{sp}^2$  center in these two systems is nearly identical ( $1.2 \text{ kcal mol}^{-1}$ ).

The formal reduction of double bonds at the rim was envisaged as a spectroscopically relevant modification of the chrysaorole ring system. Accordingly, hexahydrochrysaorole **7** was prepared by the catalytic hydrogenation of **4**, followed by the fold-in procedure (18% yield, Scheme 1). As in the case of **5**, the complete assignment of  $^1\text{H}$  and  $^{13}\text{C}$  NMR spectroscopic signals was possible for **7** by means of two-dimensional spectroscopy, and excellent correlation with the GIAO shifts was observed (Figure 5). As expected, the low-field region of the  $^1\text{H}$  NMR spectrum of **7** features only two signals, at  $\delta = 8.67$  and  $6.95$  ppm, which correspond to the hub and rim carbazole hydrogen atoms, respectively (Figure 3). The alkyl region contains the expected four signals of the butyl substituent and two higher-order multiplets at  $\delta = 4.00$  and  $3.38$  ppm, which correspond to the saturated peripheral bridge. The presence of these two resonances, marked *exo* and *endo* in Figure 3, is direct spectroscopic proof that the

chrysaorole nucleus is indeed nonplanar: a crucial piece of information that was lacking in the spectrum of **5**. The *endo* and *exo* positions are differentiated by the convex shape of the chrysaorole, and they would be exchanged by a bowl-inversion process. However, no signs of chemical exchange, either in the form of line broadening or EXSY peaks, were observed in the  $^1\text{H}$  NMR spectra of **7**, even in those recorded at 410 K in  $[\text{D}_{10}]p$ -xylene. Thus, unlike corannulene,<sup>[1b,20]</sup> hexahydrochrysaorole (and most likely chrysaorole itself) is a conformationally rigid molecule.

DFT calculations performed for **7a** ( $\text{R}=\text{H}$ ) predict a strain energy very similar to that of the parent system **5a** ( $54 \text{ kcal mol}^{-1}$ ; see the Supporting Information). DFT models obtained for the substituted system **7** show that, apart from the mobility of chains as described above for **5**, the reduced system possesses additional degrees of freedom associated with the tetrahedral centers on the rim (Figure 4). The  $\text{CH}_2\text{-CH}_2$  bridges adopt a *gauche* conformation with a CCCC torsion angle of approximately  $45^\circ$ . As a result, the surface of the bowl in **7** becomes slightly ruffled, and the molecular symmetry is lowered to  $\text{C}_3$  or  $\text{C}_1$ , depending on the relative configurations of the ethylene bridges. The *gauche* arrangement of the ethylene bridges causes further differentiation of the *endo* and *exo* hydrogen atoms into pseudoaxial and pseudoequatorial positions (Figure 4). However, the corresponding differentiation (or broadening) of  $^1\text{H}$  NMR signals was not observed in  $\text{CD}_2\text{Cl}_2$  even at 170 K; we can therefore conclude that the process of bridge inversion must be very rapid.<sup>[21]</sup> We were nevertheless able to find a link between the DFT structure and the fast-exchange NMR spectroscopic data by calculating not only chemical shifts but also the  $^1\text{H}\text{-}^1\text{H}$  coupling constants for hexahydrochrysaorole. The resulting values were averaged to account for the assumed bridge-inversion process and used to simulate the  $^1\text{H}$  NMR spectrum of **7** (Figure 3). The characteristic AA'BB' spin system of the *endo*-*exo* pair was very accurately reproduced by the calculation.

The fold-in synthesis of chrysaoroles described herein offers a potentially general route to other bowl-shaped molecules. Further investigation is needed to test its usefulness, which will depend on the identity of the coupled subunits, the size of the macrocycle, and the substitution pattern. We hope that, with further refinement, the present methodology will provide access to nonplanar aromatic compounds with unique physical characteristics.

Received: October 23, 2012

Revised: November 20, 2012

Published online: December 18, 2012

**Keywords:** density functional calculations · fused-ring systems · macrocycles · nitrogen heterocycles · NMR spectroscopy

- [1] a) G. Mehta, H. S. P. Rao, *Tetrahedron* **1998**, *54*, 13325–13370; b) Y.-T. Wu, J. S. Siegel, *Chem. Rev.* **2006**, *106*, 4843–4867; c) V. M. Tsefrikas, L. T. Scott, *Chem. Rev.* **2006**, *106*, 4868–4884; d) T. Amaya, T. Hirao, *Chem. Commun.* **2011**, *47*, 10524–10535; e) A. Sygula, *Eur. J. Org. Chem.* **2011**, 1611–1625; f) C. Thilgen,

- Angew. Chem.* **2012**, *124*, 7190–7192; *Angew. Chem. Int. Ed.* **2012**, *51*, 7082–7084.
- [2] a) W. E. Barth, R. G. Lawton, *J. Am. Chem. Soc.* **1966**, *88*, 380–381; b) R. G. Lawton, W. E. Barth, *J. Am. Chem. Soc.* **1971**, *93*, 1730–1745.
- [3] H. Sakurai, T. Daiko, T. Hirao, *Science* **2003**, *301*, 1878.
- [4] a) L. T. Scott, E. A. Jackson, Q. Zhang, B. D. Steinberg, M. Bancu, B. Li, *J. Am. Chem. Soc.* **2012**, *134*, 107–110; b) T. Amaya, T. Nakata, T. Hirao, *J. Am. Chem. Soc.* **2009**, *131*, 10810–10811.
- [5] Q. Zhang, K. Kawasumi, Y. Segawa, K. Itami, L. T. Scott, *J. Am. Chem. Soc.* **2012**, *134*, 15664–15667.
- [6] a) M. Bühl, *Chem. Eur. J.* **1998**, *4*, 734–739; b) E. Steiner, P. W. Fowler, L. W. Jenneskens, *Angew. Chem.* **2001**, *113*, 375–379; *Angew. Chem. Int. Ed.* **2001**, *40*, 362–366; c) M. A. Dobrowolski, A. Ciesielski, M. K. Cyrański, *Phys. Chem. Chem. Phys.* **2011**, *13*, 20557–20563.
- [7] A. S. Filatov, A. Y. Rogachev, E. A. Jackson, L. T. Scott, M. A. Petrukhina, *Organometallics* **2010**, *29*, 1231–1237.
- [8] See, for example: a) B. D. Steinberg, E. A. Jackson, A. S. Filatov, A. Wakamiya, M. A. Petrukhina, L. T. Scott, *J. Am. Chem. Soc.* **2009**, *131*, 10537–10545; b) K. T. Rim, M. Siaj, S. Xiao, M. Myers, V. D. Carpentier, L. Liu, C. Su, M. L. Steigerwald, M. S. Hybertsen, P. H. McBreen, G. W. Flynn, C. Nuckolls, *Angew. Chem.* **2007**, *119*, 8037–8041; *Angew. Chem. Int. Ed.* **2007**, *46*, 7891–7895; c) K. Y. Amsharov, M. A. Kabdulov, M. Jansen, *Angew. Chem.* **2012**, *124*, 4672–4675; *Angew. Chem. Int. Ed.* **2012**, *51*, 4594–4597.
- [9] a) K. Imamura, K. Takimiya, T. Otsubo, Y. Aso, *Chem. Commun.* **1999**, 1859–1860; b) Q. Tan, S. Higashibayashi, S. Karanjit, H. Sakurai, *Nat. Commun.* **2012**, *3*, 891.
- [10] E. C. Dunne, É. J. Coyne, P. B. Crowley, D. G. Gilheany, *Tetrahedron Lett.* **2002**, *43*, 2449–2453.
- [11] CCDC 906691 contains the supplementary crystallographic data for this paper. These data can be obtained free of charge from The Cambridge Crystallographic Data Centre via [www.ccdc.cam.ac.uk/data\\_request/cif](http://www.ccdc.cam.ac.uk/data_request/cif).
- [12] T. Yamamoto, A. Morita, Y. Miyazaki, T. Maruyama, H. Wakayama, Z. H. Zhou, Y. Nakamura, T. Kanbara, S. Sasaki, K. Kubota, *Macromolecules* **1992**, *25*, 1214–1223.
- [13] The name proposed for **5** reflects its resemblance to a jellyfish and the yellow color of the compound. *Chrysaora* is a genus of jellyfish from the Pelagiidae family. The genus was named after Chrysaor, Medusa's son (Χρυσάωρ, “golden armament”): F. Péron, C. A. Lesueur, *Ann. Mus. Hist. Nat.* **1809**, *14*, 325–366.
- [14] The von Baeyer name of **5** is 9,18,45-tributyl-9,18,45-triazatri-decacyclo[24.18.1.0<sup>3,42</sup>.0<sup>6,41</sup>.0<sup>8,39</sup>.0<sup>10,38</sup>.0<sup>12,36</sup>.0<sup>15,35</sup>.0<sup>17,33</sup>.0<sup>19,32</sup>.0<sup>21,30</sup>.0<sup>24,29</sup>.0<sup>27,44</sup>]pentatetraconta-1(44),2,4,6,8(39),10(38),11,13,15,17(33),19(32),20,22,24,26,28,30,34,36,40,42-heneicosane.
- [15] For a performance analysis of computational methods with respect to geodesic polyarenes, see: M. A. Petrukhina, K. W. Andreini, J. Mack, L. T. Scott, *J. Org. Chem.* **2005**, *70*, 5713–5716.
- [16] Accurate geometries are considered a prerequisite for the determination of reliable GIAO shieldings for protons in aromatic systems: C. S. Wannere, K. W. Sattelmeyer, H. F. Schaefer III, P. v. R. Schleyer, *Angew. Chem.* **2004**, *116*, 4296–4302; *Angew. Chem. Int. Ed.* **2004**, *43*, 4200–4206. For earlier GIAO calculations on bowl-shaped systems, see Ref. [8a].
- [17] This structural feature creates an analogy between chrysaoroles and kekulenes: B. Kumar, R. L. Viboh, M. C. Bonifacio, W. B. Thompson, J. C. Buttrick, B. C. Westlake, M.-S. Kim, R. W. Zoellner, S. A. Varganov, P. Mörschel, J. Teteruk, M. U. Schmidt, B. T. King, *Angew. Chem.* **2012**, DOI: 10.1002/ange.201203266; *Angew. Chem. Int. Ed.* **2012**, DOI: 10.1002/anie.201203266.
- [18] J. C. Hanson, C. E. Nordman, *Acta Crystallogr. Sect. B* **1976**, *32*, 1147–1153.
- [19] R. C. Haddon, L. T. Scott, *Pure Appl. Chem.* **1986**, *58*, 137–142.
- [20] L. T. Scott, M. M. Hashemi, M. S. Brachter, *J. Am. Chem. Soc.* **1992**, *114*, 1920–1921.
- [21] For an analogous conformational-exchange process in 9,10-dihydrophenanthrene, the inversion barrier was estimated by NMR spectroscopy to be lower than 25 kJ mol<sup>-1</sup>: R. Cosmo, S. Sternhell, *Aust. J. Chem.* **1987**, *40*, 35–47.